EEET ECOLOGICAL ENGINEERING & ENVIRONMENTAL TECHNOLOGY

Ecological Engineering & Environmental Technology 2024, 25(8), 170–182
https://doi.org/10.12912/27197050/189626
ISSN 2299–8993, License CC-BY 4.0

Received: 2024.05.22
Accepted: 2024.06.17
Published: 2024.07.01

Flood Hazard Assessment of National Road N2 Intersection with Wadi Sefrou (North East of Morocco)

Zahaf Toufik[1], Boushaba Farid[1], Mimoun Chourak[2*], Maelaynayn El Baida[1]

[1] Laboratory of Modeling and Scientific Computation, National School of Applied Sciences of Oujda, Mohamed 1st University, 60000, Morocco

[2] Laboratory of Applied Sciences, National School of Applied Sciences of Oujda, Mohamed 1st University, 60000, Morocco

* Corresponding author's e-mail: zahaf.toufik@gmail.com

ABSTRACT

The city of Bni drar in the NE of Morocco experienced frequent and regular share of flood events, especially at its main road where it's commonly submerged by floodwaters during these events. Because of its crucial significance and role in the transportation infrastructure of the region, this study aims to analyze and evaluate flood hazard in Bni Drar, with a specific focus on its impact on the national road N2 as it crosses the Sefrou wadi. Rainfall-runoff transformation was conducted using HEC-HMS model, resulting in flow hydrographs for 10, 20, 50, and 100 years return period. These hydrographs constituted an input for IBER hydrodynamic model, enabling the simulation of flood depth and velocity for a return period of 100 years. Flood hazard was categorized by taking into account both flood depth and velocity. The maximum water depth in the study area is 2.7 meters for 100 years return period. Regarding flow velocity, the maximum value is 2 meters per second. The acquired hazard maps possess the capability to bolster flood risk management within the research region by furnishing a geospatial decision support instrument to empower local authorities. This enables the prompt execution of preventive measures against flood risks and fortifies the resilience of the territory.

Keywords: Bni Drar, national road N2, Sefrou wadi, flood hazard, hazard mapping.

INTRODUCTION

Over the past three decades, natural disasters, usually considered exceptional events, have become a subject of current interest and concern for the entire international community, in a context marked by the acceleration of climate change. Natural disasters continue to increase in frequency and intensity. For example, over the period 2000–2019, no fewer than 7,348 natural disasters were recorded worldwide, an average of almost 370 per year. These disasters resulted in the tragic loss of 1.23 million human lives, an average of 61,500 deaths per year, and their economic impact was estimated at around 3.1% of global GDP (source: https://www.undrr.org/publication/human-cost-disasters-overview-last-20-years-2000-2019). In recent years, Morocco, like most countries in the world, has had to cope with natural disasters such as the Al-Haouz seism (2023), the Guelmim-Sidi Ifni floods (2014), the Al-Hoceima seism (2004), the Ourika flood (1995), which have had major repercussions on the economic, social, cultural, health and environmental impact.Although all natural hazards are of great importance, flooding is a recurrent phenomenon in Morocco, following intense rainfall that inflicts considerable damage on human lives, economies and the environment.

Examples include flooding in the Tangier-Tetouan region in March 2024, in Errachidia, Tnighir and Oujda in September 2023, and in Taroudant in 2019. Flooding stands out as a predominant natural peril in Morocco's eastern region, attributable to the shifting climate patterns and the semi-arid environment prevailing in this area (Carneiro et al., 2010). These circumstances

trigger forceful deluges, underscoring the significance of conducting similar research endeavors in this region (Grari et al., 2019; Boushaba et al., 2020; Mouzouri et al., 2013; Zahaf et al., 2021).

Flood events inflict substantial harm on human lives, economies, and the environment, with a particularly pronounced impact on transportation infrastructures. As a result, safeguarding and mitigating the risk of flooding for these critical transport networks has emerged as an imperative objective for contemporary society (Astrid et al., 2016; He et al., 2023; Zahra et al., 2019). Consequently, flood risk prevention has taken precedence on the agendas of local authorities and disaster management officials, as they endeavor to curtail the attendant human and material losses. However, it is essential to acknowledge that assessing flood risk requires a comprehensive approach (Yu et al., 2023).

In this context, a complex interplay exists between flood risk and resilience (Wang et al., 2023). Moreover, it is imperative to integrate flood risk with socio-economic vulnerability to effectively prioritize high-risk zones and devise strategies for flood prevention and management (Jibhakate et al., 2023).

Within this framework, the study's primary aim revolves around the evaluation and mapping of flood hazard in the Sefrou wadi watershed located to the south of Bni Drar city. Focusing in particular on the impact of flooding on the national road N2 as it crosses the Sefrou wadi. This road is of great importance for the oriental region, as it represents the principal road link between the city of Oujda, capital of the Oriental region, and the international airport of Angad, as well as the cities of Berkane, Saidia and Nador to the north. Stopping traffic on this road therefore has a considerable impact on the entire logistical and economic chain of the eastern region.

The study explored the contribution of geographic information systems (GIS) to natural hazard management. Combining GIS with other hydrological analysis and simulation tools will provide a powerful spatial analysis tool that empower to preclude and minimize damage, while providing vital data for informed land-use planning in the future (Sunmin et al., 2018; Sy et al., 2023; Weday et al., 2023). In our specific case, topographic data undergo processing using ArcGIS tools, while the HEC-HMS system is harnessed for watershed area analysis and hydrograph generation, duly accounting for precipitation and land-use. The latter variable assumes particular importance in flood risk assessment (Liu et al., 2023; Md Abdullah et al., 2019).

For the hydraulic simulation of flooding within the study area, the IBER model, predicated on finite volume method, is adopted. This model enjoys extensive usage in two-dimensional modeling of free-surface flows (Bladé et al., 2014; Orlando et al., 2018) and is also used for groundwater management (Kadiri et al., 2023). Leveraging the IBER flow model, the expanse of flooding is charted in terms of water depth and flowing velocity, thereby permitting the classification of flood hazard. Our present undertaking will equip the local authorities of Bni Drar, along with their partners and stakeholders, with a decision support tool, facilitating the simulation of flooding based on rainfall data, damage estimation, and the implementation of preemptive measures to mitigate flood hazard.

STUDY AREA

The Wadi Sefrou meanders through an expansive watershed encompassing nearly 170 square kilometers. Its source lies in the elevated terrains of the Béni Snassen mountain range, coursing toward the Angad plain situated to the south of Bni Drar city (Figure 1). The stream's natural channel distinctly manifests itself in the upper segments of the Angad plain. After traversing approximately ten kilometers of the Angad plain, the Wadi Sefrou loses its channel and divides into several smaller tributaries. During flood events, these tributaries inundate their surroundings, affecting the entire plain. Where the stream intersects with roads, hydraulic structures of scupper type are employed to facilitate passage.

DATA AND METHODOLOGY

Hydrological model – rainfall-runoff transformation

Within the scope of our study, we incorporated the hydrologic modeling system (HEC-HMS) for the execution of hydrological modeling. This work was made after processing the digital terrain model (DTM) using the suite of ArcGIS tools. The delineation and characterization of watersheds, coupled with the comprehensive analysis of the hydrogeometric network, was expertly conducted through the utilization of the Arc Hydro tool, as

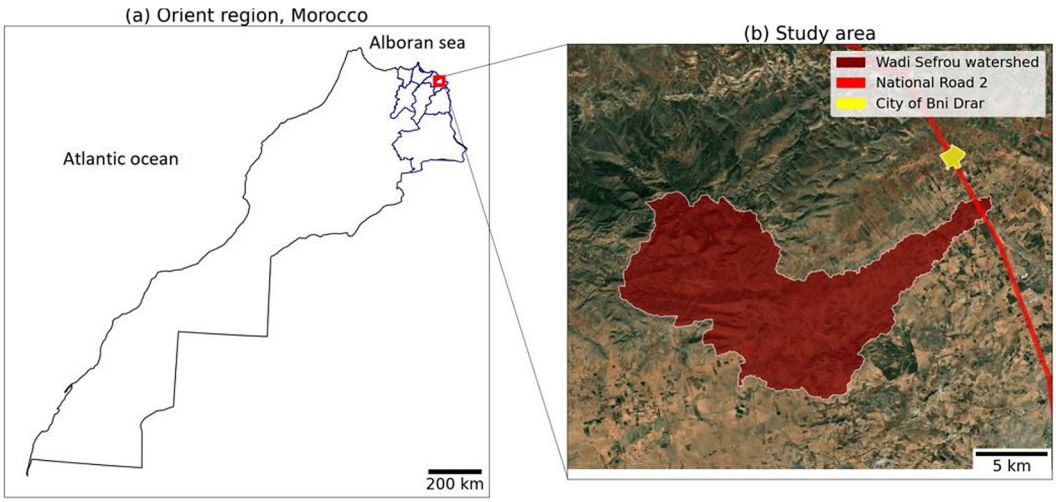

Figure 1. Location of Bni drar, national road N2, and Sefrou wadi

illustrated in Figure 2. Table 1 presents the properties of the watershed.

The compactness index is calculated using the following formula:

$$K_G = \frac{P}{2\sqrt{\pi . A}} \quad (1)$$

where: K_G – Gravelius compactness index, P – watershed perimeter (in kilometer), A – watershed area (in square kilometer).

HEC-HMS, a simple and versatile hydrological model, adapts seamlessly to a spectrum of geographical contexts. Its proven efficacy is further underscored by its prominent role in numerous contemporary research endeavors, as documented in prior works (Fernández et al., 2022; Prado et al., 2019).

In our specific investigation, we deployed HEC-HMS to orchestrate the intricate process of transforming precipitation into runoff dynamics within the confines of the study area. HEC-HMS comprises a cadre of indispensable processes, encompassing loss factors, the conversion of surplus rainfall into runoff, the infusion of base flow, and the dynamic hydrographs within the wadi bed. These derived hydrographs serve as a pivotal precursor for the IBER hydrodynamic

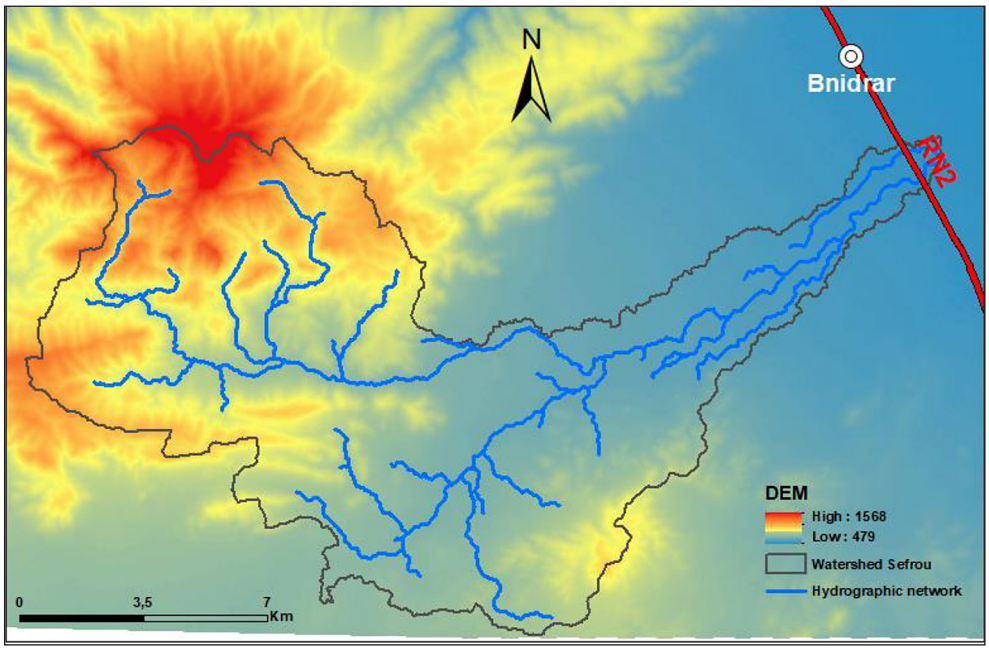

Figure 2. Watershed delineation, and its hydrographic network

Table 1. Watershed properties

Area	Length	Slope	Scope	Zmax	Zmin	Elevation	Compactness
m²	Km	%	Km	m	m	m	
170	37	20	96	1567	497	1070	2.085

model, a tool of paramount importance for the simulation of flooding events at specific return intervals. To gain comprehensive insight into the structural composition of the HEC-HMS model, reference Figure 3, an intricate visual representation elucidating the amalgamation of its constituent elements.

The Table 2 explains the HEC-HMS input data used for the net rainfall-runoff transformation. The soil conservation service (SCS) method accounts for variables such as soil class and vegetation cover as illustrated in Figure 4. Its ubiquity within analogous academic endeavors substantiates its sound scientific underpinnings (Caro-Camargo et al., 2018).

Hydraulic model

To define the equations that govern flood propagation, IBER uses Saint-Venant's model, one of the most commonly used models for

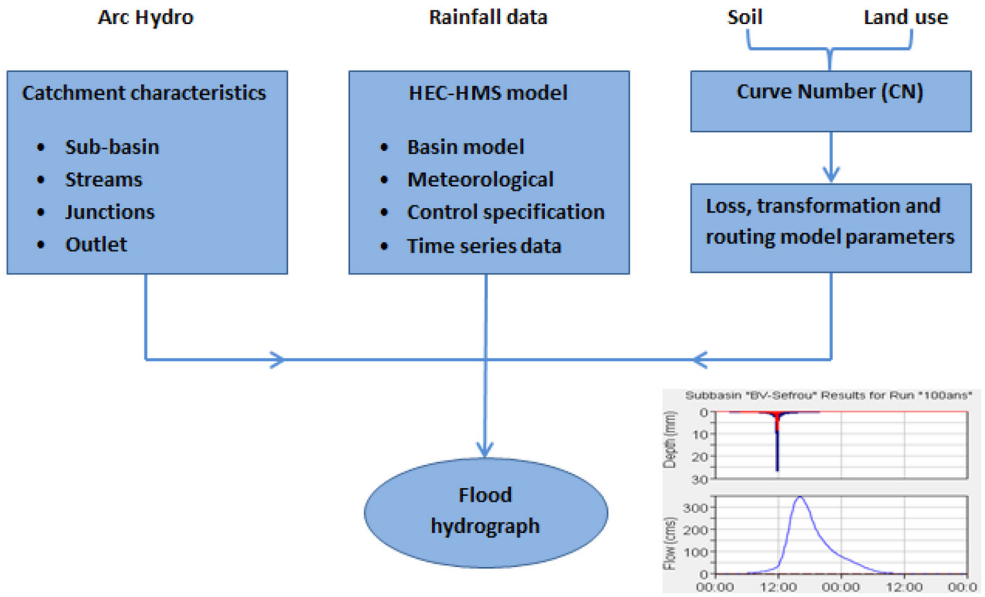

Figure 3. Flowchart of the methodology HEC-HMS

Table 2. Required data for HEC-HMS

Geometric data	Rainfall data	Rainfall losses	Transformation
The geometric data of the watershed are obtained by processing the digital terrain model on ArcGis.	• The 24-hour rainfall for the return periods considered is obtained by statistical adjustment of the rainfall data (cf. section 4.1). • The SCS type 2 storm model is adopted in the category on the typical storm model, as it corresponds to an arid zone comparable to our study area.	• Interception is considered non-existent, as the land is characterized by very little vegetation cover, • Evaporation is ignored, considering the short period of the storm, • For infiltration, the SCS method is used with a curve number value CN=80 obtained during a previous scientific survey in the proximity of the study area (Zahaf et al.2023). • The initial abstraction is considered non-existent, as the land is mostly dry.	The SCS Unit hydrograph method is adopted considering its current use in similar studies.

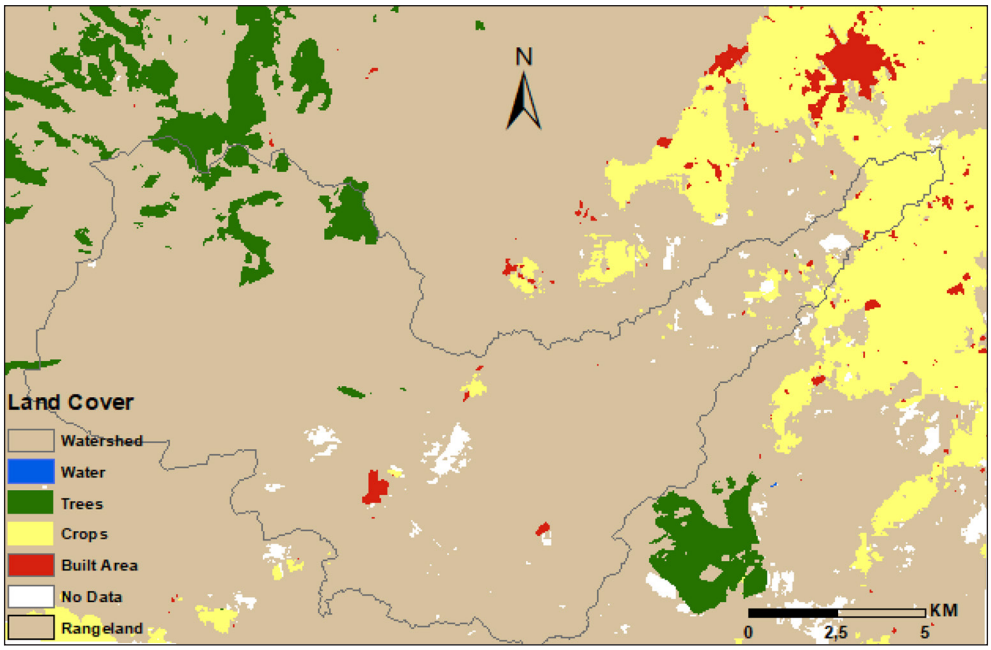

Figure 4. Land-use land-cover map

describing surface flows, built upon the laws of mass conservation (1) and motion quantity (2) and (3), integrating the turbulence and surface friction generated by the wind.

The basis of Saint-Venant's two-dimensional hydrodynamic model can be presented by the following Equations:

$$\frac{\partial h}{\partial t}+\frac{\partial hU_x}{\partial x}+\frac{\partial hU_y}{\partial y}=0 \tag{2}$$

$$\frac{\partial}{\partial t}(hU_x)+\frac{\partial}{\partial x}(hU_x^2+g\frac{h^2}{2})+\frac{\partial}{\partial y}(hU_xU_y)=$$
$$=-gh\frac{\partial z_b}{\partial x}+\frac{\tau_{sx}}{\rho}-\frac{\tau_{bx}}{\rho}+\frac{\partial}{\partial x}(\upsilon_t h\frac{\partial U_x}{\partial x})+\frac{\partial}{\partial y}(\upsilon_t h\frac{\partial U_x}{\partial y}) \tag{3}$$

$$\frac{\partial}{\partial t}(hU_y)+\frac{\partial}{\partial y}(hU_y^2+g\frac{h^2}{2})+\frac{\partial}{\partial x}(hU_xU_y)=$$
$$=-gh\frac{\partial z_b}{\partial y}+\frac{\tau_{sy}}{\rho}-\frac{\tau_{by}}{\rho}+\frac{\partial}{\partial x}(\upsilon_t h\frac{\partial U_y}{\partial x})+\frac{\partial}{\partial y}(\upsilon_t h\frac{\partial U_y}{\partial y}) \tag{4}$$

where: h – signifies water height (in meters), U_y and U_x – correspond to the average flow velocities along the y and w axes (in meters per second), g represents gravity acceleration (in meters per second squared), ρ – denotes water density (in kilograms per cubic meter), Z_b – characterizes the channel bottom elevation (in meters), τs – accounts for free surface friction due to wind, τb – encapsulates friction originating from channel bottom interactions, and 'υt' represents turbulent viscosity.

The mathematical solution of these equations is meticulously achieved by employing the finite volume method, a widely recognized and dependable approach for resolving the mathematical representation presented as a set of differential equations. In essence, this method ranks among the most prevalent and trustworthy techniques for spatial discretization. Distinguished by its theoretical foundations stemming from both the finite increment approximation and the method of finite element, the fundamental tenet of the finite volume method centers on the integrating partial differential systems over regions termed "control volumes" This approach yields a refined and straightforward solving, distinguishing it from the finite difference method, which often splits the computational area into rectangular or square cells.

A notable aspect of the finite volume method is its versatility in mesh configuration. The mesh can take on various forms, including triangular, quadrangular, or hybrid structures, and it can be structured or unstructured. This adaptability makes the finite volume method highly suitable for handling complex geometries and diverse boundary conditions.

For the boundary conditions of our Iber model, we set a 30 meters section in the outlet of the Sefrou watershed as the inlet of the discharge, in which the input values was the 100-year flood hydrograph obtained from HEC-HMS. The outlet was set at a large section covering all the land

downstream. The structured mesh type size was set to 10 meters. Land use categorization within Iber was done according to Figure 4, where its roughness values were assigned according to Manning's coefficients. The satellite image was imported from Google Maps.

The numerical schemes used in IBER to solve the hydrodynamic equations have been integrated into a powerful pre- and post-processing interface such as GiD, making this software package an efficient tool for calculating free-surface flows. A detailed description of the model, including application and validation examples, can be found in scientific research papers (Bladé et al., 2014).

Flood hazard categorization

Recognizing the inadequacy of water depth as a sole indicator of flood hazard, it's essential to acknowledge that areas characterized by high flood depths and low flow velocities may not necessarily pose a significant risk (Kvočka et al., 2016). Therefore, in the comprehensive assessment of flood hazard within the extent of our case study, our approach encompasses both flood depth and flow velocity.

Drawing inspiration from the preventive flood risk plan of the Announay commune (PPRi d'Annonay 2010), an assessment based on the values of simulated water levels and velocities for a 100-year return period was conducted. As a result, the flood hazard is classified into three distinct categories, as shown in Table 3.

RESULTS AND DISCUSSION

Flow hydrographs

The maximum daily rainfall obtained from the Moulouya hydraulic basin agency for the period 1985–2015, went through a statistical adjustment of Gumbel, giving a daily rainfall values (P_{24h}) from 10 to 100 year return period. The Gumbel distribution, long recognized as the winning model for quantifying extreme precipitation risk (Koutsoyiannis 2003), served as the fundamental framework for our statistical fit. The resulting results, covering different return periods, are presented in Table 4.

The process of breaking down or "disaggregating" the 24-hour rainfall depths into 60-minute time intervals is achieved through a hypothetical temporal distribution method, specifically the SCS Type-II approach. This method is chosen for its conservative nature, as it recognizes that the most intense rainfall events tend to occur in the middle of the storm.

The foundational hydrological model for the study area was crafted within the HEC-HMS software. This model serves as the cornerstone for the generation of runoff hydrographs at 60-minute intervals during the hydrograph construction process. Consequently, Figure 5 provides a visual representation of the simulated flood hydrographs. The resultant peak discharges for various return periods corresponding to the design storm rainfall are thoughtfully detailed in Table 5.

Flood hazard and maps

The previously established flow hydrographs have been utilized as crucial boundary conditions for input into the IBER hydraulic simulation zone. The IBER model output provides a comprehensive quantification of flooding, including information on inundation depth and water velocity. In particular, the hydraulic modelling for the centennial event, representing the most severe scenario, has delineated the areas susceptible to flooding along the course of

Table 4. 24-hour rainfall

Return period	P_{24h} in mm
10	63
20	74
50	87
100	96

Table 3. Hazard classes as a function of flood depth and velocity for a return period of 100 years, adopted from the preventive plan of flood risk of Announay commune

Hazard	0 < Depth < 1 m	1 < Depth < 2 m	2 m < Depth
Velocity < 0.5 m/s	Low hazard	Medium hazard	High hazard
0.5 m/s < Velocity < 1 m/s	Medium hazard	High hazard	High hazard
1 m/s < Velocity	High hazard	High hazard	High hazard

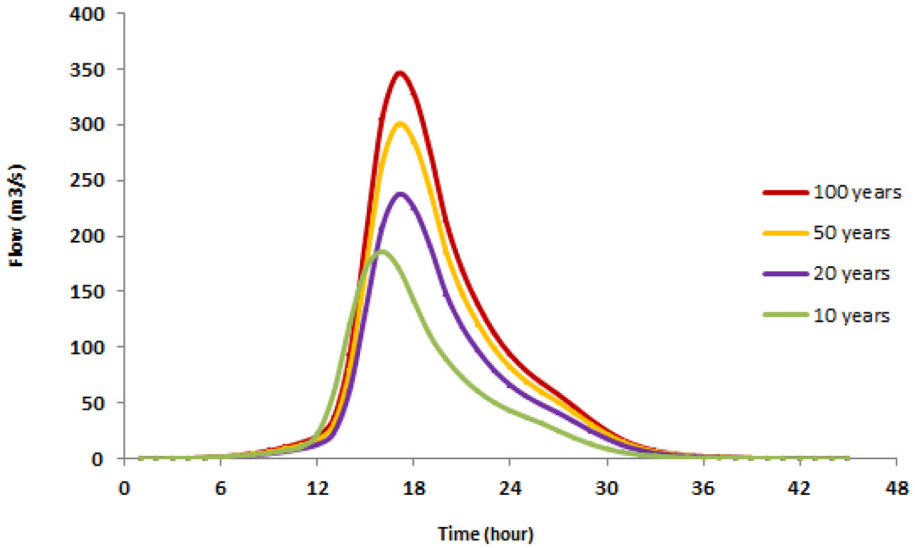

Figure 5. Flow hydrographs for 10, 20, 50 and 100 years

Table 5. Peak flows for the frequencies considered

Return period	Maximum discharge in m^3/s
10	186.1
20	237.1
50	300.5
100	346.0

the Wadi Sefrou. Figure 6 depicts a map showcasing water levels during a 100-year event, revealing significant water depths across the entire plain inundated by the Wadi Sefrou's overflow. Notably, the region where the national road N2 intersects exhibits substantial water depths, with Figure 7 confirming this observation. It showcases a 1300-meter segment of the N2 road submerged, with a maximum water depth of 2.7 meters. This situation forebodes substantial damage to the road infrastructure and the potential disruption of traffic for extended periods, ranging from hours to days. The resulted simulation results shows the flow velocity for an event corresponding to a return period of 100 years (Figure 8). High flow velocities are obtained in the area adjacent to the Wadi Sefrou bed, especially before crossing the N2 road (>2 $m \cdot s^{-1}$), and this can significantly damage road infrastructure. Taking

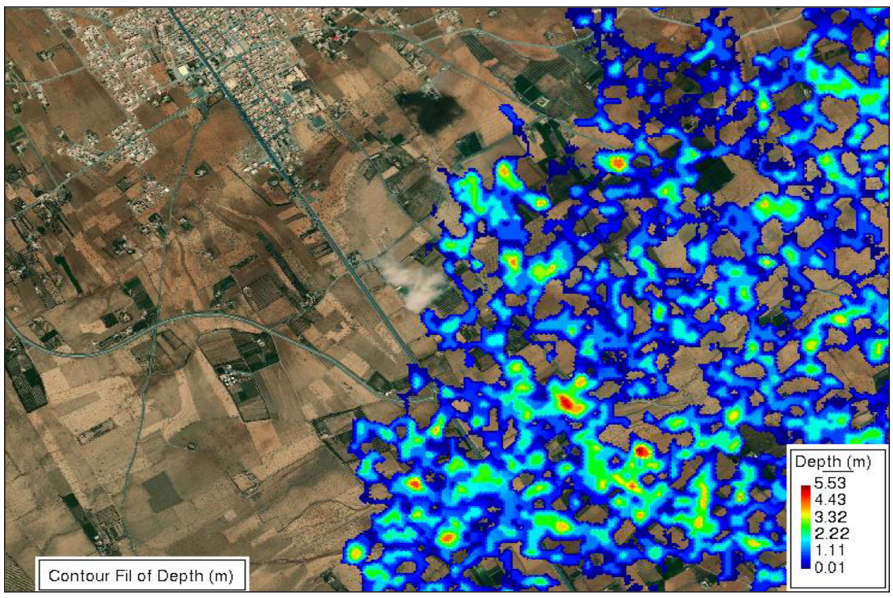

Figure 6. Inundation depth mapping for a return period of 100 years

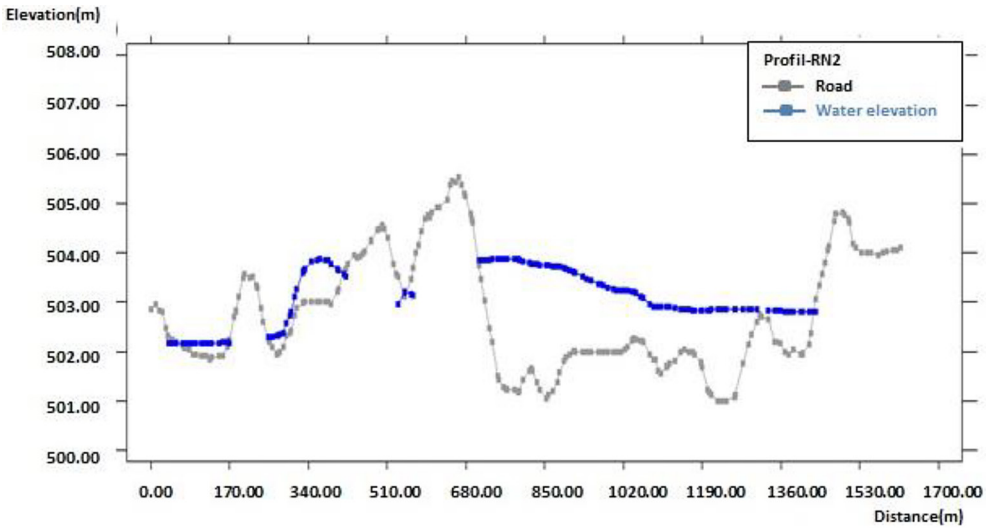

Figure 7. Profil water elevation in the intersection of national road N2 and Sefrou wadi

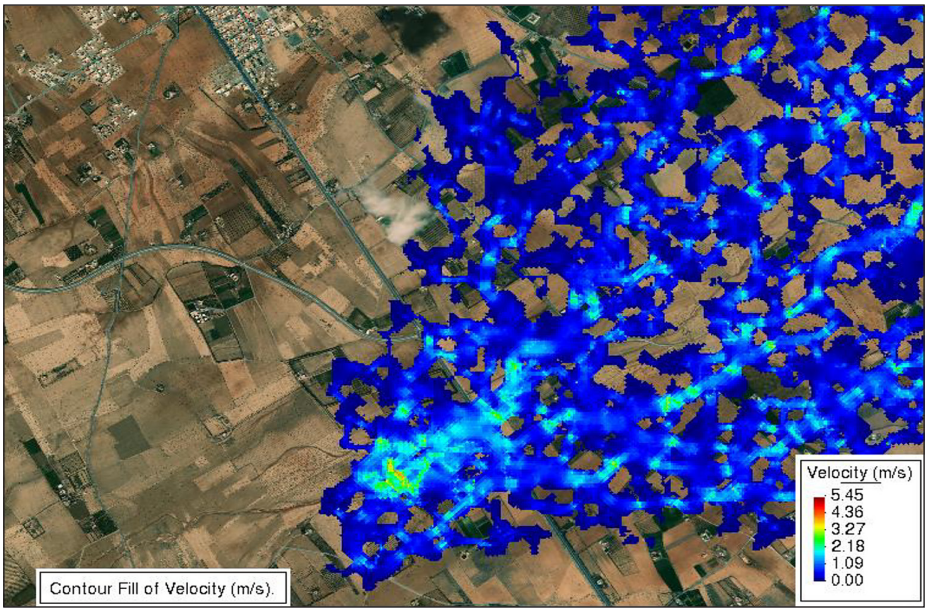

Figure 8. Velocity map for 100 years

into account the above results, the flood hazard map is drawn up to identify areas affected by or vulnerable to flooding. It is based on the superimposition of the two maps relating to water depth and flow velocity. These two criteria are categorized using table 3 and digitally incorporated to generate the hazard map, as depicted in Figure 9. According to the map of flood hazard, the national road N2 at the Sefrou wadi intersection passes through an area at high risk of flooding. It also reveals that residential areas adjacent to the N2 are categorized as medium to high risk, presenting a considerable risk to personal safety and property in this area.

Validation by real flood event and magnitude comparison with empirical methods

Being a key topic in flood risk analysis, flood hazard validation is highly advisable, as numerous factors of uncertainty impact them, as the topographic depiction and roughness parameters play a role in influencing the uncertainty associated with the modeled flood depth and velocity (Daniela et al., 2019). For our case study, with the absence of recorded up-and-downstream flow hydrographs, and remotely-sensed mapped inundation extents, our hazard maps were validated through inundation

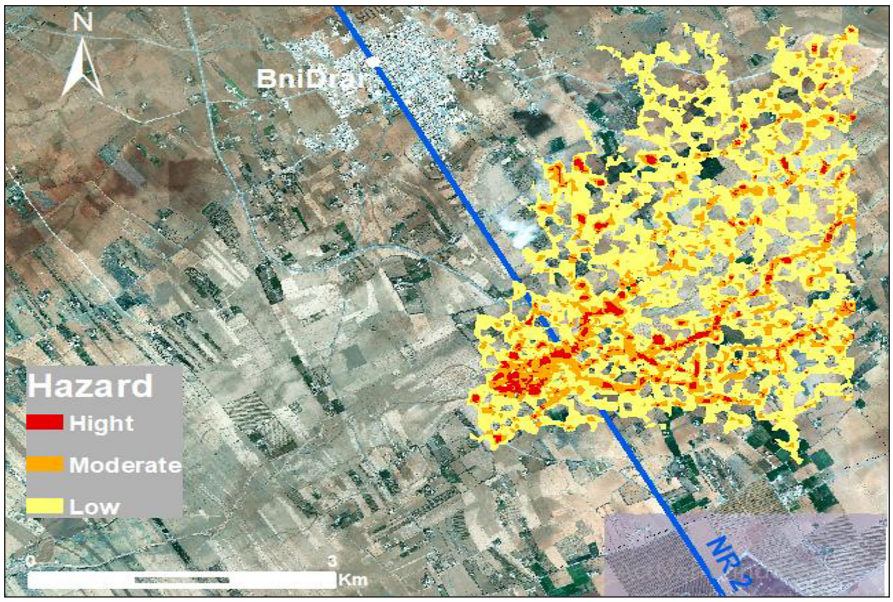

Figure 9. Hazard map for 100 years

depth measurement for a real flood event (Apel et al., 2009). In September 2nd, 2023, rainfall was recorded in the study area with a peak rainfall about 40 mm. Figure 10 shows different inundated locations affected by the mentioned event. The intersection of national road N2 and Sefrou wadi underwent an inspection the next day. The examination revealed visible traces of flooding on the resilient concrete structure (Figure 11). Notably, the vertical distance between the riverbed and the evident flood marks exceeded a 2 meters. Although the height of these marks corresponds to a rainfall that is lower than that of the 100-year return period (Table 3), it serves as a significant and acceptable comparison for validating the results of the hydraulic simulation obtained for a 100-year return period in which the flood depth reached 2.7 m. The watershed on the Sefrou wadi with an area of 170 km² is classified in the category of large watersheds (> 100 km²). The discharge values for the 100-year return period, obtained through empirical formulas used in Morocco for this type of watershed, are summarized in the Table 6.

By comparing these discharge values with the one provided by the hydrograph obtained through modeling with HEC-HMS, which is 346 m³/s, it

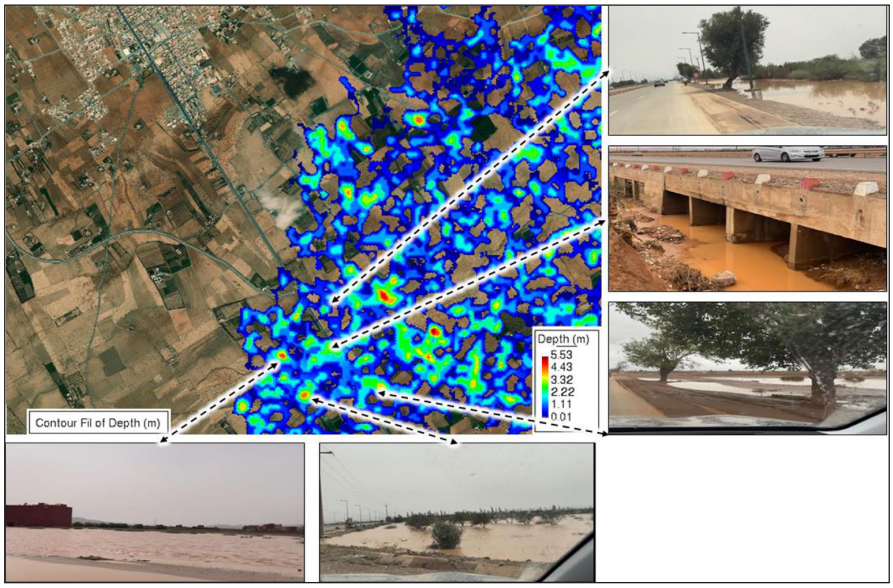

Figure 10. Iber flood depth and the locations affected by the flood of September 2nd, 2023

Figure 11. Inundation height in the intersection of national road N2 and Sefrou wadi

Table 6. Peak discharge values obtained for the Sefrou wadi watershed by empirical formulas

Method	Fuller II	Mallet-Gautier	Gradex
Discharge for 100 years (m^3/s)	325	376	363

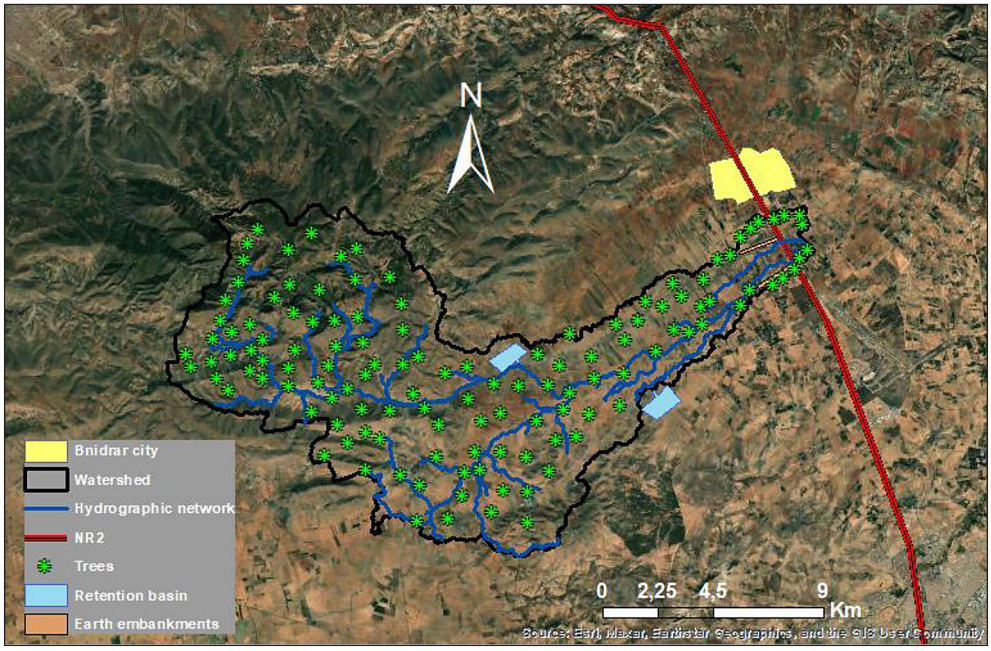

Figure 12. NBS solution map

is evident that this latter value is of the same order of magnitude as the results from the empirical formulas. This comparison thus serves as a validation of the adopted HEC-HMS hydrograph.

CONCLUSIONS

The escalation in flood frequency and intensity, attributed to the global rise in average temperatures driven by climate change, has thrust flood risk management into the forefront of our concerns. This study is a direct response to this pressing issue, focusing on the comprehensive evaluation of flood risk at the intersection of the national road N2 with Wadi Sefrou, situated to the south of Bni Drar city.

This region has encountered recurrent episodes of flooding, leading to extensive damage to infrastructure and properties in close proximity to the Wadi Sefrou watercourse. This watercourse is prominently delineated in the upper reaches of the plain but gradually dissipates towards the

middle, branching into smaller streams. The repercussions of this wadi's flooding are felt downstream, inundating the plain.

Our approach relies on the utilization of the ArcGIS geographic information system, enabling the creation of a digital terrain model for the study area. This model incorporates watershed delineation and hydrographic network treatment. Additionally, a hydrological model is meticulously developed, coupling HEC-HMS with IBER to simulate runoff. These cutting-edge technological tools have gained widespread recognition globally, serving as robust analytical instruments for the prediction of watershed hydrological behavior during flood events.

The results obtained from our study underscore the considerable vulnerability of the national road N2 at its intersection with Wadi Sefrou. Indeed, the maximum water depth in this zone is 2.7 meters for a 100-year return period, with a maximum flow velocity of 2 meters per second. Consequently, the road's infrastructure faces a high risk of damage, with the potential for traffic disruption. Notably, the national road N2 serves as a vital transport artery for this region, it links the region's principal cities to the city of Oujda, capital of the oriental region, and to the international airport of Angad, accommodating an median daily traffic volume surpassing 18,000 vehicles, according to data from the Ministry of Equipment and Water.

Furthermore, the consequences of flooding extend to residential areas in the downstream plain, situated to the south of Bni Drar's urban center, posing significant threats to the safety of residents and their property within this flood-prone zone. The study extends its impact by mapping the extent of flooding, generating detailed maps depicting water depth, flow velocity, and flood hazard categorization. The findings of the visit made to the study area the day after the rainfall on September 02, 2023 confirmed that the results obtained are plausible and significant. Our primary objective is to make substantive contributions to flood risk mitigation and the enhancement of territorial resilience.

To prevent the risk of flooding, we advocate a holistic approach that includes the application of flood hazard prevention strategies, the widespread dissemination of urbanization suitability maps, the establishment of a geographical information system for flood risk assessment, coupled with an efficient warning system, and fostering a culture of prevention within civil society. We also propose the implementation of nature-based solutions (NBS) to reduce the impact of flood risks. Indeed, researchers have recently been paying increasing attention to nature-based solutions (NBS), which can provide effective, sustainable, and cost-efficient solutions to mitigate flood risks (Jessica Penny and al., 2023; Keiko Hori et al., 2023). Nature-based solutions can help mitigate flood risks by restoring the hydrological functions of ecosystems. Nature-based solutions focus on protecting, sustainably managing and restoring natural and modified ecosystems, effectively and appropriately adapted to the local context, while benefiting both biodiversity and human well-being.

The following are some nature-based solutions that can be used for flood risk management in our case:

1. The green approach – it consists of reforestation and afforestation wich are nature-based solutions for flood risk management. Planting trees and restoring forest cover can help to reduce the runoff and soil erosion, regulate water flow, and improve soil structure. Reforestation can also provide other benefits such as carbon sequestration, biodiversity conservation, and livelihood improvement
2. Retention basin – this is an open-air rainwater storage basin. It is designed to temporarily store rainwater before discharging it at a controlled rate into a watercourse or reusing it for irrigation.
3. Earth embankments – a linear earthen structure, raised above the natural ground level, which protects against flooding of watercourses. it also guides the flow of water towards the outlet.
4. Regular cleaning of hydraulic structures under the national road N2 – this operation is essential to prevent clogging of these structures by sediment and detritus transported during floods, and to maintain their drainage capacity as well as the preservation of the environment.

The map in Figure 12 shows a typical schematic plan of NBS solutions proposed in the study area to mitigate flood risk. These recommended measures represent the principles of solutions adapted to our case, and which of course require a specific study to demonstrate their impact on reducing the risk of flooding in the study area for validation.

REFERENCES

1. Grari A., Chourak M., Boushaba F., Cherif S., García Alonso E. 2019. Numerical characterization of torrential floods in the plain of Saïdia (North-East of Morocco). Arabian Journal of Geosciences. https://doi.org/10.1007/s12517-019-4288-1

2. Michielsen A., Kalantari Z., Lyon S.W., Liljegren E. 2016. Predicting and communicating flood risk of transport infrastructure based on watershed characteristics. Journal of Environmental Management. https://doi.org/10.1016/j.jenvman.2016.07.051
3. Bladé E., Cea L., Corestein G., Escolano E., Puertas J., Vázquez-Cendón E., Coll A. 2014. Iber: herramienta de simulación numérica del flujo en ríos. Revista internacional de métodos numéricos para cálculo y diseño en ingeniería, 30(1), 1–10. https://doi.org/10.1016/j.rimni.2012.07.004
4. Boushaba F., Grari A., Chourak M., Regad Y., Elkihel B. 2021. Numerical Simulation of the Flood Risk of the Deviation Hydraulic Structure at Saidia (North-East Morocco). In: Hajji, B., Mellit, A., Marco Tina, G., Rabhi, A., Launay, J., Naimi, S. (eds) Proceedings of the 2nd International Conference on Electronic Engineering and Renewable Energy Systems. ICEERE (2020). Lecture Notes in Electrical Engineering, vol 681. Springer, Singapore. https://doi.org/10.1007/978-981-15-6259-4_68
5. Carneiro J.F., Boughriba M., Correia A., Zarhloule Y., Rimi A., El Houadi B. 2010. Evaluation of climate change effects in a coastal aquifer in Morocco using a density-dependent numerical model. Environmental Earth Sciences, 61, 241–252. https://link.springer.com/article/10.1007/s12665-009-0339-3
6. Caro-Camargo C.A., Bayona-Romero J.A. 2018. Hydro-dynamic modeling for identification of flooding zones in the city of Tunja. Revista Facultad de Ingeniería Universidad de Antioquia, 88, 40-54. https://doi.org/10.17533/udea.redin.n88a05
7. Molinari D., De Bruijn K.M., Castillo-Rodríguez J.T., Aronica G.T., Bouwer L.M. 2019. Validation of flood risk models: Current practice and possible improvements. The International Journal of Disaster Risk Reduction. https://doi.org/10.1016/j.ijdrr.2018.10.022
8. Fernández-Nóvoa D., García-Feal O., González-Cao J., DeCastro M., Gómez-Gesteira M. 2022. Multiscale flood risk assessment under climate change: the case of the Miño Wadi in the city of Ourense, Spain. Natural Hazards and Earth System Sciences, 22, 3957–3972. https://doi.org/10.5194/nhess-2022-80
9. Apel H., Aronica G.T., Kreibich H., Thieken A.H. 2009. Flood risk analyses - how detailed do we need to be. Natural hazards. https://doi.org/10.1007/s11069-008-9277-8
10. He R., Zhang L., Tiong R.L. 2023. Flood risk assessment and mitigation for metro stations: an evidential-reasoning-based optimality approach considering uncertainty of subjective parameters. Reliability Engineering & System Safety, 109453. https://doi.org/10.1016/j.ress.2023.109453
11. Penny J., Alves P.B.R., De-Silva Y., Albert S. Chen, Slobodan Djordjević, Sangam Shrestha, Mukand Babel. (2023). Analysis of potential nature-based solutions for the Mun River Basin, Thailand. Water Science & Technology. https://doi.org/10.2166/wst.2023.050
12. Jibhakate S.M., Timbadiya P.V., Pate P.L. 2023. Multiparameter flood hazard, socioeconomic vulnerability and flood risk assessment for densely populated coastal city. Journal of environmental management, 344, 118405. https://doi.org/10.1016/j.jenvman.2023.118405
13. Kadiri M., Barkoaui A.E, Zarhloule Y., Grari A. 2023. Modelling surface runoff coupling the Iber and SWMM models for groundwater recharge: case study of Tamellat plain (Morocco). Arabian Journal of Geosciences, 16(6), 397. https://link.springer.com/article/10.1007/s12517-023-11492-0
14. Keiko Hori K., Saito T., Saito O., Hashimoto S., Taki K., Yoshid T., Fukamachi K., Ochiai C. 2023. Factors motivating residents of flood-prone areas to adopt nature-based solutions for flood-risk reduction. International Journal of Disaster Risk Reduction. https://doi.org/10.1016/j.ijdrr.2023.103962
15. Koutsoyiannis D. 2003. On the appropriateness of the Gumbel distribution for modeling extreme rainfall. ESF LESC Exploratory Workshop, Hydro Risk, Bologna, Italy. http://dx.doi.org/10.13140/RG.2.1.3811.6080
16. Kvočka D., Falconer R.A., Bray M. 2016. Flood hazard assessment for extreme flood events. Nat Hazards, 84, 1569–1599. https://doi.org/10.1007/s11069-016-2501-z
17. Liu J., Xiong J., Chen Y., Sun, Zhao X., Tu F., Gu Y. 2023. An integrated model chain for future flood risk prediction under land-use changes. Journal of Environmental Management. 342, 118125. https://doi.org/10.1016/j.jenvman.2023.118125
18. Sunmin L., Saro L., Moung-Jin L., Hyung-Sup J. 2018. Spatial Assessment of Urban Flood Susceptibility Using Data Mining and Geographic Information System (GIS) Tools. https://doi.org/10.3390/su10030648
19. Md Abdullah A.B., Muktarun I., Supria P. 2019. Flood hazard, vulnerability and risk assessment for different land use classes using a flow model. Earth Systems and Environment, 4, 225–244. https://doi.org/10.1007/s41748-019-00141-w
20. Mouzouri M., Irzi Z., Essaddek A. 2013. Utilisation d'image satellitaire et d'un modèle numérique d'altitude pour la cartographie des zones à risque d'inondation sur le littoral méditerranéen de Saïdia. Rev Française de Photogrammétrie et de Télédétection, 201, 49–63. https://doi.org/10.52638/rfpt.2013.45
21. Orlando G.-F., González-Cao J., Gómez-Gesteira M., Cea L., Domínguez J.M., Formella A. 2018. An Accelerated Tool for Flood Modelling Based on Iber Water, 10, 1459. https://doi.org/10.3390/w10101459
22. PPRi d'Annonay. Dossier d'approbation : Rapport de présentation. Available online : https://

www.mairie-annonay.fr/IMG/pdf/plu_07_liste_servitudes.pdf

23. Prado-Hernández J.V., Pascual-Ramírez F., Cristóbal-Acevedo D., Valentín-Paz O.G., Sánchez-Morales J.J.F. 2019. Application of HEC-HMS and IBER in the numeric modeling of floods in the Rio San Sebastian of the municipality of Totolapan, Morelos, Mexico. Wit Transactions on Ecology and the Environment, 239, 263–274. https://orcid.org/0000-0001-6045-1661
24. Sy H.M., Luu C., Bui Q.D., Ha H., Nguyen D.Q. 2023. Urban flood risk assessment using Sentinel-1 on the google earth engine: A case study in Thai Nguyen city, Vietnam. Remote Sensing Applications: Society and Environment, 31, 100987. https://doi.org/10.1016/j.rsase.2023.100987
25. Wang Y., Zhang C., Chen A.S., Wang G., Fu G. 2023. Exploring the relationship between urban flood risk and resilience at a high-resolution grid cell scale. Science of The Total Environment, 164852. https://doi.org/10.1016/j.scitotenv.2023.164852
26. Weday, M.A., Tabor, K.W., Gemeda, D.O. 2023. Flood hazards and risk mapping using geospatial technologies in Jimma City, southwestern Ethiopia. Heliyon, 9(4). https://doi.org/10.1016/j.heliyon.2023.e14617
27. Yu J., Zou L., Xia J., Chen X., Wang F., Zuo L. 2023. A multi-dimensional framework for improving flood risk assessment: Application in the Han Wadi Basin, China. Journal of Hydrology: Regional Studies, 47, 101434. https://doi.org/10.1016/j.ejrh.2023.101434
28. Zahaf T., Hichame S., Farid B., Chourak M. 2023. Mapping the risk of flooding of the national road N° 2 at the crossing of the wadi Tamdmadt north of the city of Bni Drar. Materials Today: Proceedings, 72, 3447–3453. https://doi.org/10.1016/j.matpr.2022.08.089
29. Zahaf I., Chourak B. 2021. Risk of flooding of the national road N° 6 at the right of crossing the wadi Asla in the region of Taourirt. Materials Today: Proceedings, Elsevier. https://doi.org/10.1016/j.matpr.2021.03.484
30. Kalantari Z., Santos Ferreira C.S., Koutsouris A.J., Anna-Klara Ahlmer A.-K., Artemi Cerdà, Georgia Destouni. 2019. Assessing flood probability for transportation infrastructure based on catchment characteristics, sediment connectivity and remotely sensed soil moisture. Science of the Total Environment. https://doi.org/10.1016/j.scitotenv.2019.01.009